arXiv:nlin/0507023v2 [nlin.CD] 11 Aug 2006

Topological Chaos in Spatially Periodic Mixers

Matthew D. Finn, Jean-Luc Thiffeault,* and Emmanuelle Gouillart

Department of Mathematics, Imperial College London, SW7 2AZ, United Kingdom

(Dated: March 30, 2022)

Topologically chaotic fluid advection is examined in two-dimensional flows with either or both directions spatially periodic. Topological chaos is created by driving flow with moving stirrers whose trajectories are chosen to form various braids. For spatially periodic flows, in addition to the usual stirrer-exchange braiding motions, there are additional topologically-nontrivial motions corresponding to stirrers traversing the periodic directions. This leads to a study of the braid group on the cylinder and the torus. Methods for finding topological entropy lower bounds for such flows are examined. These bounds are then compared to numerical stirring simulations of Stokes flow to evaluate their sharpness. The sine flow is also examined from a topological perspective.

PACS numbers: 47.52.+j, 05.45.-a
Keywords: chaotic advection, topological chaos

I. INTRODUCTION

We study topological chaos in regimes where two-dimensional flow is driven by moving stirrers, such as in a prototypical batch stirring device [1, 2] illustrated in Figure 1. We consider the effect of extra stirrer motions that are possible when the fluid domain has spatial periodicity. For the mixer in Figure 1, we imagine removing one or both pairs of opposite walls and identifying these edges to make a periodic domain. Our study is motivated by the many model flows examined in the literature that have spatial periodicity, such as the ubiquitous sine flow [3]. Some laboratory experiments are also designed to have spatial periodicity in one direction [4], and the square patterns formed in thermal convection exhibit periodicity in two directions [5]. There are also signal analysis applications of braid groups [6] where measured quantities can be periodic.

Topological chaos (TC) can be used to design mixers with a robust built-in stirring quality that depends only on the relative motions of the stirrers and is independent of fluid properties such as compressibility or viscosity [1]. This mixing quality can be guaranteed because stirrers are topological obstacles to flow: if their trajectories form an intertwined braiding pattern, then by continuity material lines in the fluid must also be braided. If the stirrer motion traces a braid with positive topological entropy, then typical material lines in the mixing region of the fluid will grow exponentially. Roughly speaking, this means that the braiding motion of the stirrers guarantees a minimum amount of chaos in the flow in a region around the stirrers, and chaos leads to efficient fluid mixing [7]. In the two-dimensional flows studied here, the topological entropy is related to the time-asymptotic exponential growth rate of material lines. Since the length of material lines increases rapidly, they must fold back

*Electronic address: jeanluc@imperial.ac.uk

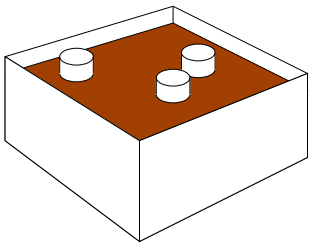


FIG. 1: The prototype batch stirring device. This bounded mixer may be made spatially periodic by removing either or both pairs of opposite walls and identifying the edges of the fluid. When this is done, extra stirrer motions are possible that traverse the periodic directions. Vertical flow effects are neglected.

and forth within the bounded mixing region and lead to the familiar "striations" observed in typical mixing flows.

The properties of a braid are linked to Thurston–Nielsen theory [8, 9]. Thurston proved that a two-dimensional homeomorphism (here, the map giving the motion of fluid particles in one period) can be decomposed into regions that are either reducible, finite-order, or isotopic to a pseudo-Anosov map. Braids are a convenient language to describe the *isotopy classes* of these homeomorphisms. For our purposes, the third type is most important: pseudo-Anosov maps have strong chaotic properties and typically lead to good mixing. If the braid is *irreducible* with positive entropy, then to it must correspond a region of the flow that is a single chaotic component. In fluid mixing parlance, this region will be well-mixed (though it could be very small or even have zero measure).

To guarantee positive topological entropy in a nonperiodic domain, it can be shown that at least three trajectories must be involved in a braid. However, this does not imply that mixers must have three or more stirrers to produce TC [10, 11]. This is because we can consider trajectories of anything that acts as a topological obstacle to material lines: in a two-dimensional flow this could be a fluid particle itself, or an entire island of regularity. Thus, all mixers generally produce TC, since it is easy to find sets of periodic trajectories that braid. This means that topological ideas can also be used to understand mixing, even for flows with fewer than three stirrers [10, 11]. It is also instructive to note that all chaos in time-periodic two-dimensional flows is topological, in the sense that the topological entropy of a flow can be arbitrarily well-approximated by considering the braiding motion of a sufficiently high-order periodic orbit [8, 12].

We begin in Section II by summarising current techniques that have been applied to bounded flows (or spatially-nonperiodic flows on the infinite plane). Then in Section III we describe ways of extending these methods for spatially periodic flows, examining in turn the case of single- and double-periodicity. In Section IV we determine the sharpness of theoretical topological entropy estimates compared to entropies for model Stokes flows. We apply our techniques to the sine flow in Section V, where the "stirrers" are given by periodic orbits. Finally, we close with a discussion of our results in Section VI.

II. BRAIDING IN A NONPERIODIC DOMAIN

In this section we describe how motion of stirrers around each other in a nonperiodic domain (*i.e.*, a surface of genus zero such as a bounded domain or the infinite plane) may be described as a braid. We then review how this braid may be used to produce a rigorous lower bound on the topological entropy of the flow. We consider two-dimensional flows, where the topological entropy is the time-asymptotic growth rate of material lines [13, 14]. (It is the supremum over all possible smooth material lines, but in practice we find that the growth rate rapidly becomes independent of the choice of initial material line, except for pathologically bad choices.)

A. Artin's Braid Group

In flows without spatial periodicity, braiding is conventionally characterised by recording exchanges of position of adjacent stirrers [1]. Stirrer positions are projected onto an axis (we have chosen the x-axis in what follows) and ordered from 1 to n along this line. If stirrer i and $i+1$ exchange order in a clockwise direction, we assign to this motion the braid group generator σ_i; an anti-clockwise crossing is labelled σ_i^{-1}. The numbers 1 to n always refer to the relative position of the stirrers along the x-axis, and do not always label the same stirrer. The procedure of associating trajectories with braid generators is explained in detail in Refs. [11, 15]. Any motion of stirrers then corresponds to an ordered sequence of generators: this sequence is an element of Artin's braid group [16, 17] on n strands. This group contains all braids generated by sequences of $\sigma_1, \ldots, \sigma_{n-1}$ and their inverses. The group operation is the catenation of braids, and the inverse is found by reversing the sequence and inverting the generators. The identity of the braid group is simply n parallel strands. We use the convention that braid generators occur from left to right, so that in the braid word $\sigma_1\sigma_2$ the generator σ_1 occurs first.

Some braids are topologically equivalent because they can be continuously deformed into each other. In fact, equivalence of braids can be established using just the group relations

$$\sigma_i\sigma_j\sigma_i = \sigma_j\sigma_i\sigma_j \qquad \text{if} \qquad |i-j| = 1, \tag{1a}$$

$$\sigma_i\sigma_j = \sigma_j\sigma_i \qquad \text{if} \qquad |i-j| \geq 2, \tag{1b}$$

which together form a presentation for the group (a minimal set of relations describing the group). Relation (1a) implies that particular sequences of three braid elements are equivalent, and is obvious by inspecting a diagram of the braid [17]. Relation (1b) dictates that any two braid events involving different pairs of stirrers can be commuted.

The braid word describing the relative motions of the stirrers encodes a great deal of information about the fluid flow. One such piece of information is the topological entropy of the braid, which is a lower bound on the topological entropy of the flow. Two methods of calculating this lower bound have been considered: matrix representations of the braid group [1, 18], and train-tracks [19]. For three stirrers, the two are equivalent; for more than three stirrers the matrix method only gives a lower bound on the topological entropy of the braid. Hence in this paper we shall use exclusively train-tracks to compute the topological entropy of a braid. This is discussed in the following sections.

B. Train-tracks

A complicated but robust method for computing braid topological entropies is the Bestvina–Handel train-track algorithm [19]. This algorithm requires the construction of a special invariant graph for each braid. Computerised implementations of this algorithm exist that take a word in generators of Artin's braid group as an input [20, 21]. These are not currently well-suited to the periodic domains that we consider here, though they could be adapted for this purpose. Here we shall be dealing with braids that are simple enough that we will not need the Bestvina–Handel algorithm. Rather, we will use the method that Thurston calls 'iterate and guess,' which is based on the fact that under iteration almost any curve converges to the train-track (for pseudo-Anosov braids).

A train-track consists of a set of edges, joined together at junctions. For the braids studied in this paper the following types of edge are needed:

1. Edges that wrap tightly around the stirrers in a closed loop starting and finishing at the same junction;

2. Edges that join the junctions associated with different stirrers.

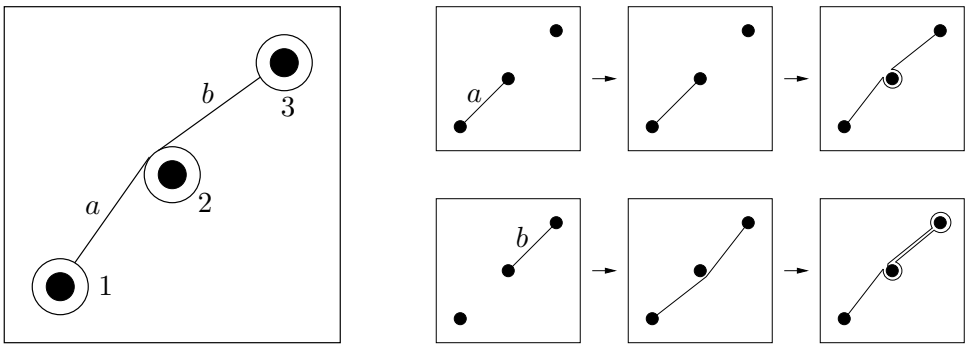
The edges of a train-track graph are deformed under the action of the braid, and we assume the edges are like elastic bands, so that they stretch by the smallest amount possible without crossing through any of the stirrers.

Type 1 edges, since they are wrapped tightly around the stirrers, are not stretched under the action of the braid. However, under the action of the braid the stirrers may be permuted, so Type 1 edges are permuted. Type 2 edges are non-trivially deformed under the braid and may become wrapped around several stirrers.

A graph is said to be invariant if under the action of the braid all edges are mapped onto edge-paths of the original graph. In general, Type 2 edges are mapped onto a edge-paths made up of Type 1 and Type 2 edges. Under the action of the flow, a material line representing edges from the train-track must be stretched at least as much as the train-track itself. However, in general it is stretched even more due to the presence of additional periodic orbits which act as obstacles to the flow (more on this in Section VI).

To summarise the technique so far: A graph of Type 1 and 2 edges is drawn between and around the stirrers. Then the stirrers are made to undergo the braid operation under investigation, and the deformation of the graph is tracked as if its edges were rubber bands. The goal is to find a graph that is invariant under the action of the braid—that is, the edges may stretch and fold, but they all end up at positions where there was initially an edge-path. Of course, the edges get permuted and stretched, so a single edge may be mapped to a path that traverses the original edges several times. We call the invariant graph a train-track for the braid. (In order to be a genuine train-track, a graph must have a special non-cancellation property that we discuss below.)

Once the train-track graph has been found, the stretching in the train-track may be measured by constructing a transition matrix describing for each edge the edge-path into which it is mapped. The logarithm of the largest eigenvalue of this matrix is the topological entropy of the braid. The largest eigenvalue is used because it is assumed that the braid operation is repeated a large number of times, so the graph converges to an invariant pattern corresponding to the eigenvector of the largest eigenvalue. The entries in the eigenvector describe the relative number of edges that accumulate under repeated action of the braid.



(a) (b)

FIG. 2: (a) The train-track for the braid $\sigma_1\sigma_2^{-1}$; (b) The deformation of edges a and b under the action of the braid.

The eigenvalue then describes the growth of the length of this invariant pattern at each application of the braid.

As an example we consider the well-studied pigtail braid $\sigma_1\sigma_2^{-1}$ with three stirrers, with train-track illustrated in Figure 2(a). It consists of three Type 1 edges, labelled 1, 2 and 3, that pass around each of the stirrers, and two Type 2 edges, labelled a and b, that join adjacent stirrers. The two sequences shown in Figure 2(b) illustrate the fate of the edges a and b under σ_1 followed by σ_2^{-1}. Up to a deformation that does not change the topology, the edges of the train track are mapped to the following edge-paths:

$$a \mapsto a2b, \quad b \mapsto a2b3b, \quad 1 \mapsto 3, \quad 2 \mapsto 1, \quad 3 \mapsto 2. \tag{2}$$

An important feature to note in this example is that ultimately the edges a and b stretch from the first stirrer, *underneath* the second one, to the third one; hence the resultant edge-paths include a tour around edge 2.

In every train-track all edges must be mapped to an edge-path that has alternately Type 2 edges (denoted by letters) and Type 1 edges (denoted by numbers). This ensures that two or more adjoining Type 2 edges do not collapse back to a shorter edge-path under repeated action of the braid. (This is the non-cancellation property alluded to above.) With no possibility of such cancellations a transition matrix can be written down by recording the number of edges in each edge-path. This matrix can then be used to determine the evolution of an arbitrary edge-path under any number of subsequent applications of the braid.

The transition matrix for the braid word $\sigma_1\sigma_2^{-1}$ is found from (2) to be

$$M = \left[\begin{array}{cc|ccc} 1 & 1 & 0 & 0 & 0 \\ 1 & 2 & 0 & 0 & 0 \\ \hline 0 & 0 & 0 & 1 & 0 \\ 1 & 1 & 0 & 0 & 1 \\ 0 & 1 & 1 & 0 & 0 \end{array}\right], \tag{3}$$

where the element M_{ij} represents the number of occurences of the ith edge in the image of the jth edge, and the indices i and j take values $(a, b, 1, 2, 3)$, in that order. Let the vector $(n_a, n_b, n_1, n_2, n_3)^T$ contain the number of edges of each type in a path. Under the action of the braid these will be mapped to a longer path with edges given by $M \cdot (n_a, n_b, n_1, n_2, n_3)^T$.

The topological entropy of the flow is given in two dimensions by the time-asymptotic growth rate of material lines (maximised over all possible smooth lines). Since the train-track could be considered as a material line, the growth rate of the flow must be at least as large as the growth rate of the train-track. This is given by the spectral radius (the magnitude of the largest eigenvalue) of the transition matrix, because for a large number of repeated applications of the braid the coiling will become dominated by the largest eigenvector of the transition matrix.

For the pigtail braid, the matrix (3) has a spectral radius of 2.62. Hence the topological entropy of the braid $\sigma_1\sigma_2^{-1}$ is $\log 2.62 \approx 0.96$. Any time-periodic flow which has material obstacles executing this braiding motion necessarily has a topological entropy of at least 0.96.

Note that since Type 1 edges are wrapped tightly around stirrers, and are only permuted amongst themselves under the braid, they do not contribute to growth of material lines. It is thus usual to write the transition matrix only for Type 2 edges. In the present example this is the upper-left block indicated in (3).

III. BRAIDING ON THE CYLINDER AND TORUS

In this section we study the braid group on the cylinder and the torus. Because of the possibility of stirrers going around the periodic direction(s), these groups are different to Artin's braid group discussed in Section II. Note that Thurston–Nielsen theory has been considered before on the annulus and torus, see for example [22] and [23]. Here we focus on a braid description of stirrer motion on these surfaces, using for the most part the notation of Birman [24].

A. Braid Groups on Periodic Domains

For a periodic domain, in addition to the braid elements σ_i representing the exchange of stirrer positions, we introduce extra motions corresponding to stirrers making tours of the periodic directions, as illustrated in Figure 3. In a singly-periodic domain we allow the extra braid motions τ_i corresponding to the ith stirrer touring the periodic direction. The singly-periodic case represents flow on a (possibly infinite) cylinder. In this paper we choose the periodicity of the cylinder to be in the x-direction without loss of generality. For a doubly-periodic flow we allow the extra braid motions τ_i and ρ_i—the additional motions ρ_i correspond to the ith stirrer touring the second periodic direction. The doubly-periodic case can be thought of as flow on a torus.

The braiding motions τ_i and ρ_i are not independent of the σ_i nor each other, since some braids can be continuously deformed into each other. The braid group relations for an arbitrary number of stirrers have been stated by Birman [24]. As an example, for the braid group on the torus with two stirrers, the one relation required to determine equivalence of braids is [24]

$$\sigma_1^2 = \rho_1^{-1}\tau_2\rho_1\tau_2^{-1}. \tag{4}$$

The relation (4) provides a presentation for the two-strand braid group on the torus, with generators $\{\sigma_1, \rho_1, \tau_2\}$. The other two operations can be written $\rho_2 = \sigma_1\rho_1\sigma_1$, $\tau_1 = \sigma_1\tau_2\sigma_1$.

The ideas developed in the following section apply for an arbitrary number of stirrers, but we shall illustrate flow with just two stirrers. We will see that is possible to create topological chaos on a periodic domain with fewer than three stirrers.

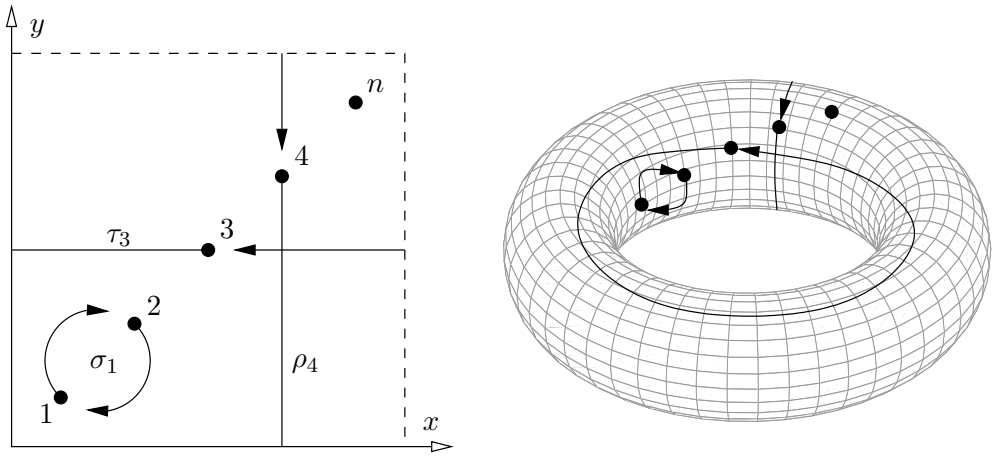


FIG. 3: Braiding operations on the cylinder and torus. In addition to the usual σ_i, corresponding to interchanging adjacent stirrers, there are new braiding operations corresponding to stirrers making a tour around one or both periodic directions. For domains that are periodic in only one direction (cylinder) we allow the generators τ_i. For doubly-periodic domains (torus) we also consider the generators ρ_i.

B. Representation for the Cylinder

For the special case of the cylinder, we consider braids formed from σ_i and τ_i generators only, and ignore ρ_i for the moment. The dynamics on a singly-periodic domain is only a little more complicated than the dynamics in a bounded domain. This is because, as pointed out in Ref. [25], there exists a conformal mapping from the periodic strip (*i.e.*, the cylinder) to an annulus, and the topological entropy of a flow is preserved under this conformal mapping.

In Figure 4 we show the result of conformally mapping the square in the z-plane (with $z = x + iy$) in Figure 3 under the mapping $w = \exp(2\pi\imath z)$ onto an annulus in the w-plane. The stirrers aligned along a diagonal are mapped onto a logarithmic spiral in the w-domain. The key feature in this w-domain is that there is a hole (centered on the origin) that acts as an $(n+1)$th stirrer. In the case of the z-domain extending to $y \to +\infty$ this hole shrinks to a point, but it is still a topological obstacle to the flow. If the z-domain includes $y \to -\infty$ then the w-domain extends to infinity.

Braid elements σ_i do not involve the hole. However, the periodic motions τ_i make a clockwise tour of the hole (stirrer $n+1$), also crossing all stirrers $i+1, \ldots, n$ twice (Figure 4). Thus the braid group on a singly-periodic domain with n strings, with generators $\{\sigma_i, \tau_1\}$, can be associated with the braid group in the plane with $n+1$ strings, with generators $\{\Sigma_i\}$, if we assign

$$\sigma_i \mapsto \Sigma_i\,, \quad \tau_i \mapsto \Sigma_i \ldots \Sigma_n \Sigma_n \ldots \Sigma_i. \tag{5}$$

An important consequence of the hole acting as a stationary stirrer is that only two proper stirrers are required to guarantee topological chaos. (On a nonperiodic domain, at least three stirrers are needed, since the topological entropy of all braids on two strands is zero [1].)

We illustrate this for the two-stirrer braid $\tau_1\sigma_1$ which is equivalent to the three-stirrer planar braid $\Sigma_1\Sigma_2\Sigma_2\Sigma_1\Sigma_1$. We will show in the following section that this braid has a topological entropy of 1.32. Note that this is larger than the entropy 0.96 for the same length

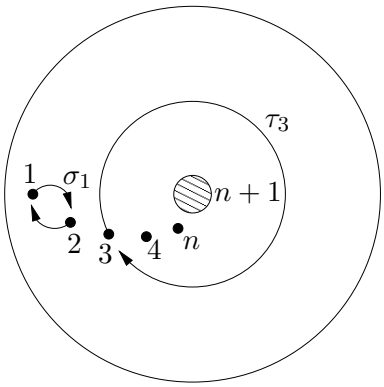


FIG. 4: Plot of the complex w-plane after making the conformal mapping $w = \exp(2\pi\imath z)$ from a singly-periodic domain with n stirrers to an annular domain. The central region (shaded) acts as an $(n+1)$th stirrer. The braid element τ_i corresponds to the ith stirrer making a clockwise tour of all the stirrers $i+1, \ldots, n+1$, so that $\tau_i \mapsto \Sigma_i \ldots \Sigma_n \Sigma_n \ldots \Sigma_i$.

braid word $\sigma_1\sigma_2^{-1}$, which was shown in Ref. [26] to be optimal on a nonperiodic domain. This suggests that periodic boundary conditions contribute significantly in creating chaos!

C. Train-tracks for the Cylinder and Torus

In principle we can compute the topological entropy of braids on the cylinder by first applying the conformal transformation defined in Section III B and finding the corresponding braid word on the annulus. However, the braid word on the annulus is usually considerably longer than that on the cylinder, which makes the train-track harder to compute. Moreover, for the doubly-periodic case (torus) there is no such conformal mapping trick, so in any case we will need to find train-tracks on periodic domains. Fortunately we can find train-tracks directly for the cylinder and torus by considering graphs with edges that traverse the periodic directions. The periodic train-tracks shown in this paper are determined by inspection, following Thurston's 'iterate and guess' approach, though we expect that existing computer codes (see *e.g.* [21]) could be extended to automate their construction.

The method works as follows. Consider stretching an elastic band between two stirrers, possibly traversing the periodic direction in doing so. Now consider the fate of the elastic under the action of the braid. The band will be stretched around the stirrers with the same topology as the train-track for the braid (except for possible rare choices of initial condition where the band undergoes a periodic motion without stretching at all). If an invariant train-track exists then the elastic band will tend to align with it as it is stretched. The reason it must align is that initially the elastic crosses the train-track a fixed number of times (possibly zero), and by determinism it must still cross the same number of times even after many applications of the braid. Now, if the elastic is rapidly stretching but never makes any additional crossings of the train-track, then it must align and be stretched parallel to the track. After a few iterations of the braid it is usually possible to determine the shape of the required invariant graph by inspection. It can then be verified that the graph is a proper train-track by checking that all Type 2 edges are mapped onto edge-paths consisting of alternating Type 2 and Type 1 edges.

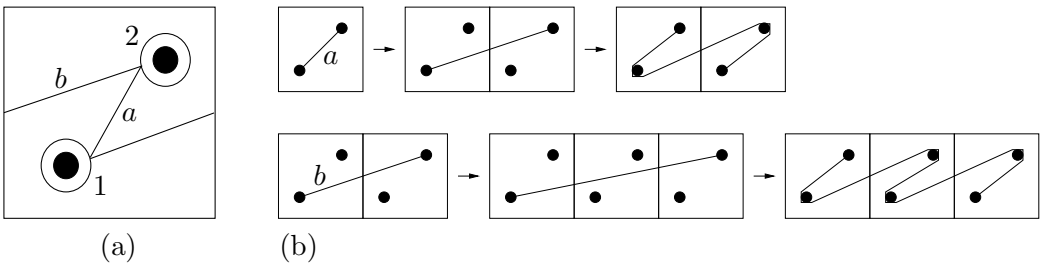


FIG. 5: (a) Train-track for the braid $\tau_1\sigma_1$ on the cylinder; (b) The deformation of edges a and b under the action of the braid.

In Figure 5 we illustrate construction of a train-track for the braid $\tau_1\sigma_1$ studied above. The starting point for this calculation is to compute the fate of an elastic band a stretched directly between the two stirrers. Under the action of the braid this is deformed into a 'Z' shape, shown in the top sequence in Figure 5(b). Note that headaches can be spared by drawing extra copies of the periodic domain as necessary, rather than attempting to wrap the line around on a single copy of the domain. The resulting 'Z' shape has two edges like the original a, and a new edge—call it b—joining stirrer 1 to 2 across the periodic direction.

The bottom sequence in Figure 5(b) shows the evolution of b. The edge b is mapped to a double 'Z' shape that spans three copies of the domain and consists of three a edges and two b edges. Because no unfamiliar edges are generated we conjecture that a and b, plus two Type 1 loops to allow lines to wrap around the stirrers, are all that is required for the train-track. To confirm that this invariant graph is a proper train-track we examine the edge-paths produced by the braid, which are

$$a \mapsto a1b2a, \quad b \mapsto a1b2a1b2a, \quad 1 \mapsto 2, \quad 2 \mapsto 1. \tag{6}$$

All the Type 2 edges are mapped to paths of alternating Type 2 and Type 1 edges, so this confirms we have found the required train-track. The transition matrix for the braid $\tau_1\sigma_1$ (ignoring Type 1 edges which do not contribute to stretching) is then

$$\begin{bmatrix} 2 & 3 \\ 1 & 2 \end{bmatrix} \tag{7}$$

with spectral radius 3.73, so the braid has a topological entropy of 1.32.

The same inspection method works for toroidal braids, where we allow the additional braid elements ρ_i corresponding to stirrers touring the second periodic direction. We illustrate the construction in Figures 6–7 for the more complicated braid $\tau_1\sigma_1\rho_1^{-1}\sigma_1$. Figure 6 depicts the invariant train-track for this braid. The action of the braid on the various edges is shown in Figure 7. Our initial 'guess' elastic band is labelled a. Under the action of the braid, a is mapped onto three new edges, b, c, and d (Figure 7, top). Edge b is mapped to a path containing b, c and d. Edge c is mapped onto b and d. Edge d is mapped onto a, b and d, and no unfamiliar edges are generated. Hence a, b, c and d, plus two small loops around the stirrers, may be checked as a candidate train-track.

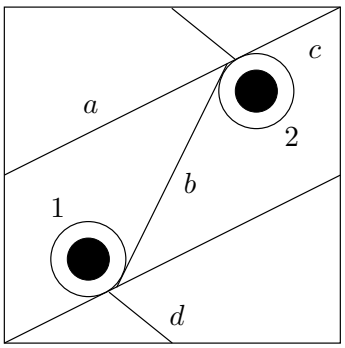


FIG. 6: The train-track for the braid $\tau_1\sigma_1\rho_1^{-1}\sigma_1$ on the torus.

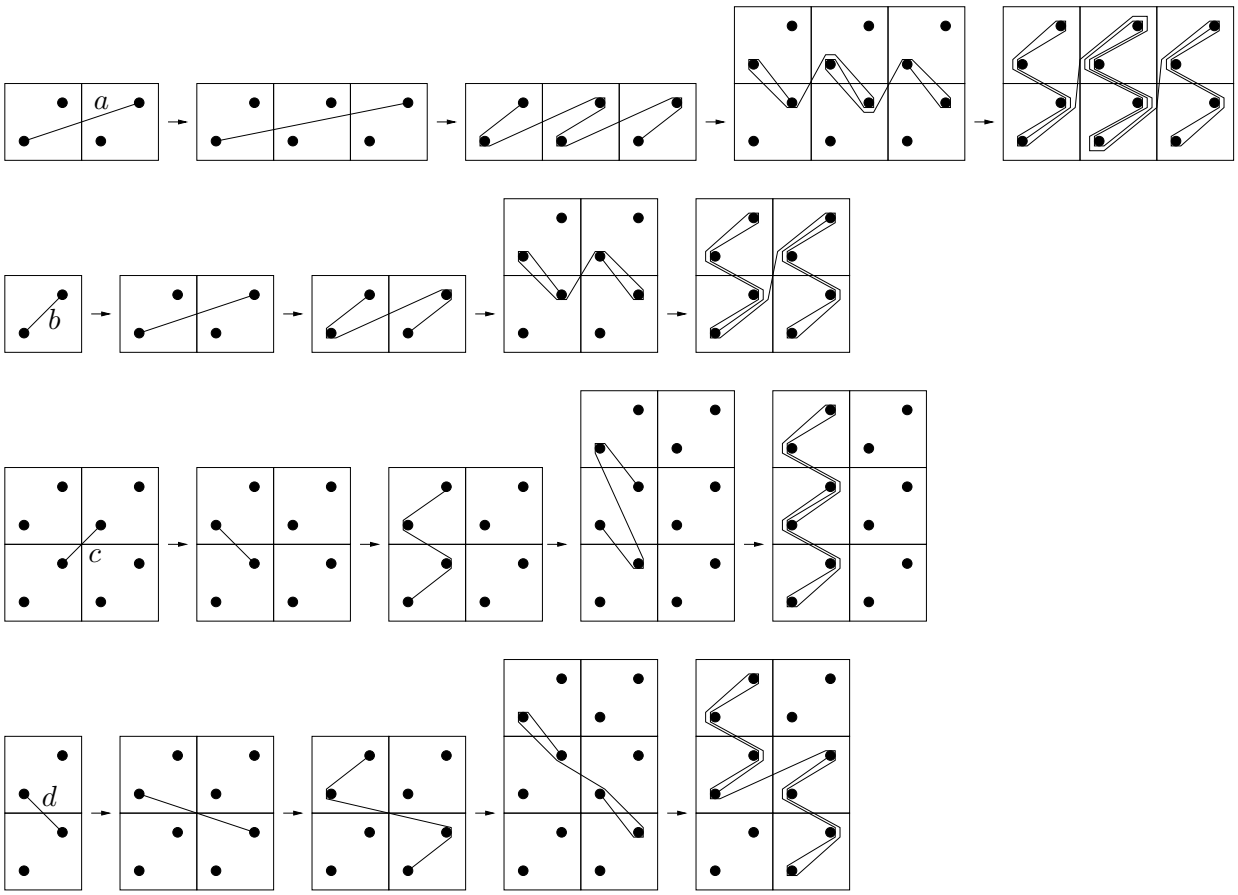


FIG. 7: The deformation of edges a, b, c, d in Figure 6 under the action of the braid $\tau_1\sigma_1\rho_1^{-1}\sigma_1$.

Careful inspection reveals edges are mapped to edge-paths as

$$\begin{aligned}
a &\mapsto b2d1b2b1d2b1b2c1b2b1d2b1b2d1b2b1d2b1b2c1b2b1d2b1b2d1b,\\
b &\mapsto b2d1b2b1d2b1b2c1b2b1d2b1b2d1b,\\
c &\mapsto b2d1b2b1d2b1d2b1b2d1b,\\
d &\mapsto b2d1b2b1d2b1a2b1d2b1b2d1b,\\
1 &\mapsto 1, \qquad 2 \mapsto 2.
\end{aligned}$$

Each of these is of the required form (that is, Type 1 edges alternate with Type 2), so this is the required train-track. The corresponding transition matrix (keeping only the finite-length Type 2 edges) for $\tau_1\sigma_1\rho_1^{-1}\sigma_1$ is then

$$\begin{bmatrix} 0 & 0 & 0 & 1 \\ 18 & 10 & 7 & 8 \\ 2 & 1 & 0 & 0 \\ 7 & 4 & 4 & 4 \end{bmatrix} \tag{8}$$

with spectral radius 14.48, so the braid has a topological entropy of 2.67. This growth rate is slightly greater than that achieved by performing the cylinder braid $\tau_1\sigma_1$ twice (resulting topological entropy 2.63), at the same energetic cost (by symmetry). However, no attempt has been made at optimising this torus braid, so braids with higher topological entropy may exist.

IV. NUMERICAL SIMULATIONS

In this section we show numerical simulations of quasi-steady two-dimensional spatially periodic Stokes flow to determine the sharpness of predicted entropy lower bounds compared to actual flow topological entropies.

Before investigating a particular flow regime, it is important to remember that the topological entropy bounds given above are based only on the braiding motion of the stirrers and are independent of all properties of the underlying fluid flow except for continuity. In a given flow regime, however, we expect that there could be additional features that lead to more intricate braiding, and therefore to an improved topological entropy.

In our simulations, entropies are computed numerically by recording the stretched length $L(t)$ of a material line as a function of time t. Because material lines are stretched exponentially fast in a chaotic flow, the slope of a best-fit line through $\log L(t)$ versus t gives the topological entropy of the flow (after ignoring initial transients).

We consider a very viscous (Stokes) fluid in a unit square domain $0 \le x, y < 1$. Stirring is performed with just two stirrers, since we have shown above that this is sufficient to allow topological chaos in a periodic domain. The stirrers are circular with diameter 1/10, and are initially centred at $(\frac{1}{4}, \frac{1}{4})$ and $(\frac{3}{4}, \frac{3}{4})$. In the stirring operations σ_1, τ_1 and ρ_1 the stirrer trajectories we prescribe are given in Table I. Note that in the Stokes flow regime the resultant advection depends only upon the paths of the stirrers and not on the stirrer velocities.

The Stokes flow velocity field was computed using the lattice-Boltzmann method [27]. Whilst a lattice-Boltzmann code is relatively inefficient for computing Stokes flow, it copes

TABLE I: Trajectories of the stirrers in the simulations corresponding to the braid generators, with $0 \leq \alpha < 1$ and $\theta = \left(\frac{1}{4} - \alpha\right)\pi$.

generator	stirrer 1	stirrer 2
σ_1	$\left(\frac{1}{2} - \frac{1}{2\sqrt{2}}\cos\theta, \frac{1}{2} - \frac{1}{2\sqrt{2}}\sin\theta\right)$	$\left(\frac{1}{2} + \frac{1}{2\sqrt{2}}\cos\theta, \frac{1}{2} + \frac{1}{2\sqrt{2}}\sin\theta\right)$
τ_1	$\left(\frac{1}{4} - \alpha, \frac{1}{4}\right) \mod 1$	$\left(\frac{3}{4}, \frac{3}{4}\right)$
ρ_1	$\left(\frac{1}{4}, \frac{1}{4} - \alpha\right) \mod 1$	$\left(\frac{3}{4}, \frac{3}{4}\right)$

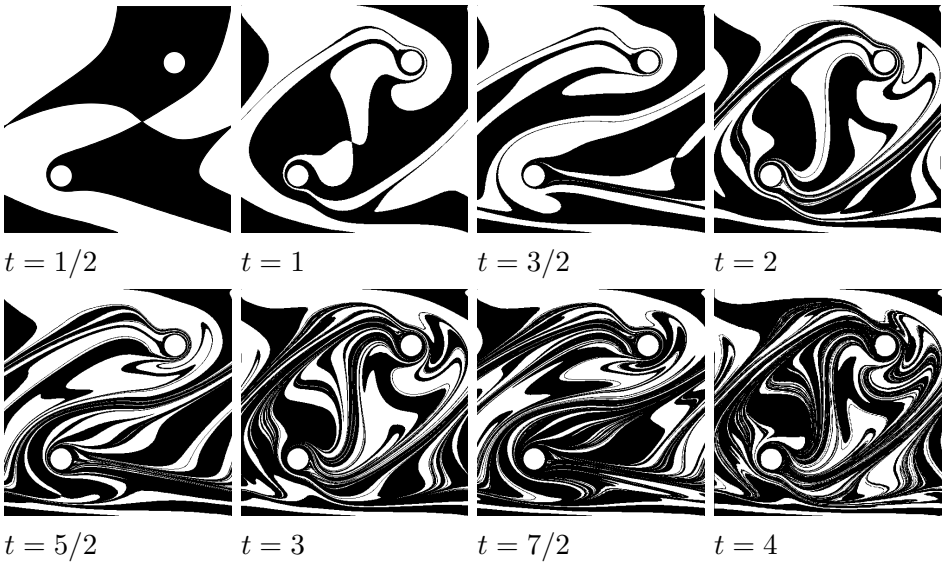


FIG. 8: Time-periodic stirred flow on the cylinder under the braid $\tau_1\sigma_1$. Each snapshot represents a half-period.

easily with the moving circular boundaries and also with periodic boundary conditions, in addition to allowing investigation of similar flows at moderate Reynolds number (not reported here). We have chosen to compute the velocity field this way because the complex variable series solution approach employed by Finn *et al.* [2] does not generalise easily for periodic domains. In computing the velocity field, for simplicity we impose a spatially periodic pressure field, and thus find the unique solution that has no net flux in either of the periodic directions.

We consider passive advection of an initial closed polygon with corners at $(0, 0)$, $(\frac{1}{2}, 0)$, $(\frac{1}{2}, 1)$, $(1, 1)$, $(1, \frac{1}{2})$ and $(0, \frac{1}{2})$, with a total length of $L(0) = 4$. This represents the interface between a two-by-two checkerboard pattern of black and white squares of fluid. As the interface is advected we use a particle insertion scheme to ensure that stretches and folds remain well resolved [28].

In Figure 8 we show the result of stirring using the braid $\tau_1\sigma_1$ in a domain that is periodic in the x-direction, with no-slip boundaries at $y = 0, 1$. Figure 9 shows the evolution of the fluid under the braid $\tau_1\sigma_1\rho_1^{-1}\sigma_1$ in a doubly-periodic domain.

In both figures it is clear that the fluid is well mixed. Closer inspection of the snapshots after complete application of each braid also reveals accumulations of thin striations that

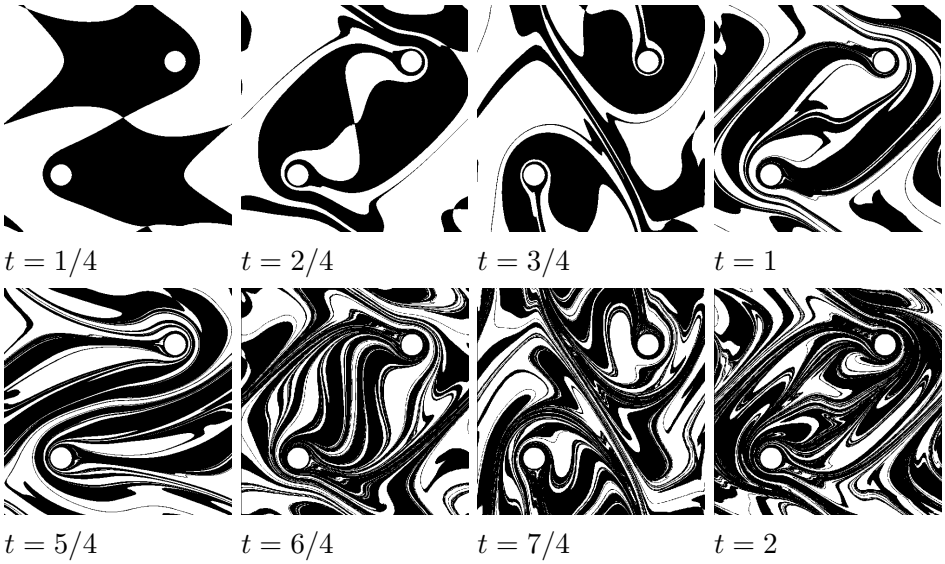


FIG. 9: Time-periodic stirred flow on the torus under the braid $\tau_1\sigma_1\rho_1^{-1}\sigma_1$. Each snapshot represents a quarter-period.

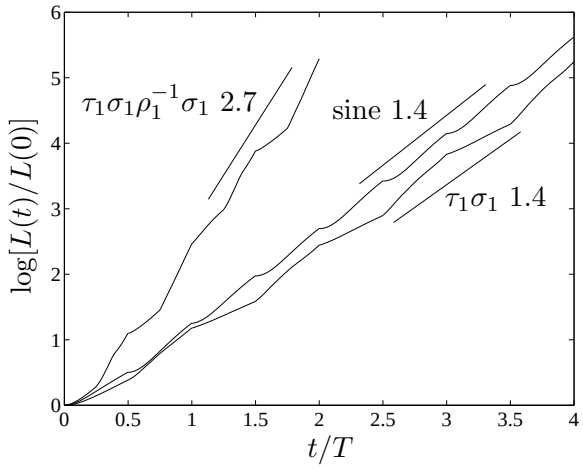


FIG. 10: Interface length for all the model flows. Plot of interface length versus time for braids in Figures 8 and 9. The length is shown on a log scale. The slope of each curve for large time gives the topological entropy of each flow.

roughly align with the train-track graph. This is more obvious for the singly-periodic case shown in Figure 8, where the thinnest striations form in a 'Z' shape similar to that shown in the corresponding train-track in Figure 5. It was noted by Alvarez *et al.* [29] that in chaotic flows striations accumulate with different densities in different regions of the domain. Here, in the long-time limit the relative number of striations caught between stirrers is given by the entries of the dominant eigenvector of the train-track transition matrix. This relative number is slightly different from the density, which depends on the size of the domain and could be locally nonuniform, but it should correlate well with it. We have not attempted to verify this, since it would require a separate study.

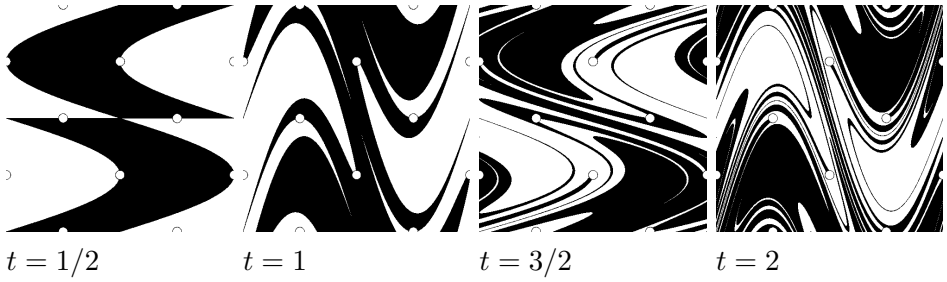


FIG. 11: Sine flow advection simulations. Each snapshot represents a half-period. The circles denote periodic orbits, with period 2.

To quantify the mixing in our two model flows we calculate numerically their topological entropies. Figure 10 shows the interface length $L(t)$ for the two flows in Figures 8 and 9. The curves quickly reach an exponential growth regime, though there is clearly some variation in growth rate during each period of the flow. To allow for this we calculate the slope of the curves from a linear least-squares fit, ignoring transient data in the first period of the flow. There is clearly some subjectivity about how such a fit is performed, so we claim our slopes are accurate to within ten percent. We find that the $\tau_1\sigma_1$ flow has an entropy of $1.4 \pm 10\%$, so the lower bound of 1.32 derived in Section III, based only on the braiding of the stirrers, is around 90% sharp. For the doubly-periodic braid $\tau_1\sigma_1\rho_1^{-1}\sigma_1$ our numerically computed entropy is around $2.7 \pm 10\%$, meaning that the lower-bound of 2.67 is at least 90% sharp. The sharpness of the bounds indicates that the braiding motion of the stirrers in our two model flows are responsible for almost all of the chaos, and only a small amount of chaos is due to secondary effects such as periodic orbits.

V. THE SINE FLOW

The fact that fluid particles themselves act as topological obstacles to flow in two dimensions [11] means that rigorous topological entropy lower bounds can be computed even when stirring apparatus is not present to force a braiding motion. To provide an illustration we consider the well-known sine flow [3], which has not been examined from such a topological perspective.

The doubly-periodic sine flow is defined on the unit square $0 \leq x, y < 1$. We consider, for simplicity, the case where the velocity field has a temporal period of unity, with the velocity field given by $(\sin 2\pi y, 0)$ for $0 \leq t < \frac{1}{2}$ and $(0, \sin 2\pi x)$ for $\frac{1}{2} \leq t < 1$. It is easy to verify that in this case the trajectories of the initial points $(\frac{1}{4}, 0)$, $(\frac{3}{4}, 0)$, $(\frac{1}{4}, \frac{1}{2})$, $(\frac{3}{4}, \frac{1}{2})$, $(0, \frac{1}{4})$, $(0, \frac{3}{4})$, $(\frac{1}{2}, \frac{1}{4})$ and $(\frac{1}{2}, \frac{3}{4})$ are all periodic, with period 2.

Figure 11 shows the result of advecting the initial condition described in Section IV according to the sine flow. It is easy to see from this numerical simulation that the trajectories of these points form a non-trivial braid. One way of writing this braid is $\sigma_1\sigma_2^{-1}\tau_4^{-1}\sigma_3^{-1}\sigma_2^{-1}\sigma_1^{-1}\sigma_7\sigma_6^{-1}\tau_5\sigma_5^{-1}\sigma_6^{-1}\sigma_7^{-1}\rho_3^{-1}\sigma_2\rho_6\sigma_6$. Note how highly-curved folds of the interface form around some of the periodic points, showing that these points really do act like small stirrers! This can occur because these are parabolic points with a singular unstable manifold, allowing material lines to fold around the point. The nature of these points and the folding behaviour will be addressed in future work.

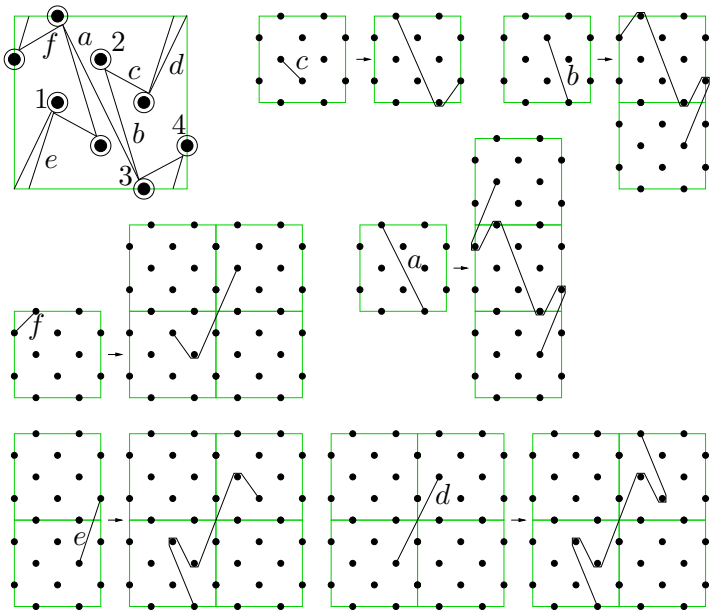


FIG. 12: Train-track for the sine Flow.

In Figure 12 we show the construction of the train-track for this braid, calculated in the same way as described in Section III. The snapshots of material lines in Figure 11 are again invaluable in determining the train-track. The edge to edge-path mapping is

$$
\begin{aligned}
&a \mapsto e4f3a3f4e,\\
&b \mapsto f3a3f4e,\\
&c \mapsto a3f,\\
&d \mapsto b2c1d1c2b,\\
&e \mapsto b2c1d1c,\\
&f \mapsto c1d,\\
&1 \mapsto 3, \quad 2 \mapsto 4, \quad 3 \mapsto 1, \quad 4 \mapsto 2,
\end{aligned}
$$

with the corresponding transition matrix

$$
\begin{bmatrix}
1 & 1 & 1 & 0 & 0 & 0\\
0 & 0 & 0 & 2 & 1 & 0\\
0 & 0 & 0 & 2 & 2 & 1\\
0 & 0 & 0 & 1 & 1 & 1\\
2 & 1 & 0 & 0 & 0 & 0\\
2 & 2 & 1 & 0 & 0 & 0
\end{bmatrix}
\tag{9}
$$

having a spectral radius of 3.38 and topological entropy 1.22. Advection of material lines in this flow can be computed quickly using a map, rather than solving the full flow numerically, therefore we can compute $L(t)$ for larger t and subsequently estimate the entropy more accurately at around 1.48. So the train-track bound is a reasonable 82% sharp, to within a percent. This bound is slightly less sharp than for the examples shown in Section IV.

Perhaps this is to be expected since we did not force the flow to execute a particular 'good' braid. Instead, we chose periodic orbits that were easily identified analytically. However, the bound could easily be improved by including further periodic points in the train-track calculation [10]. We leave this for a future study.

VI. DISCUSSION

We have shown how to compute lower bounds on the topological entropy of a two-dimensional time- and spatially-periodic fluid flow using the 'iterate and guess' approach for constructing train-tracks. For both one and two periodic directions this approach may be applied directly by considering graphs embedded on a cylinder or torus. An alternative approach may be used for singly-periodic flows, where a conformal transformation leads to a braid in an annular domain with equal topological entropy. In the latter approach, performing the conformal mapping introduces an additional flow obstacle which leads to a braiding motion with an additional, fictitious, stationary stirrer. This confirms that in a spatially periodic flow it is possible to create topological chaos with just two actual stirrers, rather than the three required in a bounded or non-periodic infinite flow [1]. The possibility of topological chaos also follows from the existence of badly-ordered periodic orbits of the circle map associated with the stirrer motion, which implies positive entropy [30].

Note that it does not follow that TC can be produced with a single stirrer on a doubly periodic domain. The toroidal braid group with one stirrer is simply $\{\tau_1, \rho_1\}$ (no σ's). These two elements commute with each other [24], so it is not possible to generate a non-trivial braid. Intuitively, with only one stirrer there is nothing to wrap the stirrer around and hence it is impossible to tangle fluid lines around anything. Flows with one stirrer can of course still be chaotic, with a finite topological entropy, but topological considerations with just one stirrer trajectory reveal nothing.

The train-track approach actually provides more information than just the growth rate of material lines. The entries in the transition matrix eigenvector corresponding to the largest eigenvalue reveal where edges in the train-track are accumulated at large times. In general the entries in this vector are different from each other and account for the spatial inhomogeneity in the relative number of striations between the stirrers, analogous to the situation described by Alvarez *et al.* [29].

In model Stokes flow simulations we have shown for the braids $\tau_1\sigma_1$ and $\tau_1\sigma_1\rho_1^{-1}\sigma_1$ the computed entropy bounds are around 90% sharp. These bounds are surprisingly good given that they are based only on the braid performed by the imposed stirrer motions, however they could be made even sharper by including information about other, secondary, periodic structures in the flow [8, 10].

We found that the topological entropy of braids on the cylinder and torus was quite high. This is not surprising: the periodic boundary conditions offer many more opportunities for complex braiding motions than the plane or a bounded domain, thus causing material lines to grow rapidly.

Using the methods presented here, it was relatively simple to find braids in the sine flow that have positive topological entropy. The fact that this topological entropy was 82% sharp when compared to the measured topological entropy of the sine flow means that much of the observed chaos is embodied in these orbits. All these orbits are parabolic, which allows folding of material lines around them—an important mechanism for chaos.

Acknowledgments

Thanks to Toby Hall for help with train-tracks, to Igor Mezić for helpful discussions, and to an anonymous referee for clarifying several aspects of Thurston–Nielsen theory. This work was funded by the UK Engineering and Physical Sciences Research Council grant GR/S72931/01.

---

[1] P. L. Boyland, H. Aref, and M. A. Stremler, "Topological fluid mechanics of stirring," J. Fluid Mech. **403**, 277 (2000).

[2] M. D. Finn, S. M. Cox, and H. M. Byrne, "Topological chaos in inviscid and viscous mixers," J. Fluid Mech. **493**, 345 (2003).

[3] R. T. Pierrehumbert, "Tracer microstructure in the large-eddy dominated regime," Chaos Solitons Fractals **4**, 1091 (1994).

[4] M. S. Paoletti and T. H. Solomon, "Experimental studies of front propagation and mode-locking in an advection-reaction-diffusion system," Europhys. Lett. **69**, 819 (2005).

[5] S. Chandrasekhar, *Hydrodynamic and Hydromagnetic Stability* (Dover, New York, 1981).

[6] A. Amon and M. Lefranc, "Topological signature of deterministic chaos in short nonstationary signals from an optical parametric oscillator," Phys. Rev. Lett. **92**, 094101 (2004).

[7] H. Aref, "Stirring by chaotic advection," J. Fluid Mech. **143**, 1 (1984).

[8] P. L. Boyland, "Topological methods in surface dynamics," Topology Appl. **58**, 223 (1994).

[9] W. Thurston, "On the geometry and dynamics of diffeomorphisms of surfaces," Bull. Am. Math. Soc. **19**, 417 (1988).

[10] E. Gouillart, M. D. Finn, and J.-L. Thiffeault, "Topological mixing with ghost rods," Phys. Rev. E **73**, 036311 (2006).

[11] J.-L. Thiffeault, "Measuring topological chaos," Phys. Rev. Lett. **94**, 084502 (2005).

[12] A. Katok, "Lyapunov exponents, entropy and periodic orbits for diffeomorphisms," Inst. Hautes Etudes Sci. Publ. Math. **51**, 137 (1980).

[13] J. M. Franks and M. Handel, "Entropy and exponential growth of π_1 in dimension two," Proc. Amer. Math. Soc. **102**, 753 (1988).

[14] S. Newhouse and T. Pignataro, "On the estimation of topological entropy," J. Stat. Phys. **72**, 1331 (1993).

[15] A. Vikhansky, "Chaotic advection of finite-size bodies in a cavity flow," Phys. Fluids **15**, 1830 (2003).

[16] J. S. Birman, *Braids, Links, and Mapping Class Groups*, *Annals of Mathematics Studies* (Princeton University Press, Princeton, NJ, 1975).

[17] K. Murasugi, *Knot theory and its applications* (Birkhäuser, Boston, 1996).

[18] B. Kolev, "Entropie topologique et représentation de Burau," C. R. Acad. Sci. Sér. I **309**, 835 (1989), english translation available at `http://arxiv.org/abs/math.DS/0304105`.

[19] M. Bestvina and M. Handel, "Train-tracks for surface homeomorphisms," Topology **34**, 109 (1995).

[20] P. Brinkmann, "An implementation of the Bestvina–Handel algorithm for surface homeomorphisms," Experiment. Math. **9**, 235 (2000).

[21] T. Hall, *Train: A C++ program for computing train tracks of surface homeomorphisms*, `http://www.liv.ac.uk/maths/PURE/MIN_SET/CONTENT/members/T_Hall.html`.

[22] P. Boyland, "An analog of Sharkovski's theorem for twist maps, " in *Hamiltonian dynamical systems (Boulder, CO, 1987)*, Vol. 81 of *Contemp. Math.* (Amer. Math. Soc., Providence, RI, 1988), pp. 119–133.

[23] J. Llibre and R. S. MacKay, "Rotation vectors and entropy for homeomorphisms of the torus isotopic to the identity," Ergod. Th. Dynam. Sys. **11**, 115 (1991).

[24] J. S. Birman, "On braid groups," Comm. Pure Appl. Math. **22**, 41 (1969).

[25] P. Boyland, M. Stremler, and H. Aref, "Topological fluid mechanics of point vortex motions," Physica D **175**, 69 (2003).

[26] D. D'Alessandro, M. Dahleh, and I. Mezić, "Control of mixing in fluid flow: A maximum entropy approach," IEEE Transactions on Automatic Control **44**, 1852 (1999).

[27] S. Chen and G. D. Doolen, "Lattice Boltzmann method for fluid flows," Annu. Rev. Fluid Mech. **30**, 329 (1998).

[28] T. S. Krasnopolskaya, V. V. Meleshko, G. W. M. Peters, and H. E. H. Meijer, "Mixing in Stokes flow in an annular wedge cavity," Eur. J. Mech. B/Fluids **18**, 793 (1999).

[29] M. M. Alvarez, F. J. Muzzio, S. Cerbelli, A. Adrover, and M. Giona, "Self-similar spatiotemporal structure of intermaterial boundaries in chaotic flows," Phys. Rev. Lett. **81**, 3395 (1998).

[30] R. S. MacKay and C. Tresser, "Badly ordered orbits of circle maps," Math. Proc. Camb. Phil. Soc. **96**, 447 (1984).